Experimental Investigation of Spruce Wood in Different Material-Directions and Constitutive Modelling Including Knot Effects

Martin FLEISCHMANN, Josef EBERHARDSTEINER, Lubomir ONDRIS

Institute for Strength of Materials, Vienna University of Technology

Adolf-Blamauer-Gasse 1-3, A-1030 Vienna, Austria, http://www.fest.tuwien.ac.at

TU VIENNA

Overview

For the development of a constitutive material model for spruce wood different types of experiments are required. During the 1990s a test series on clear spruce wood subjected to biaxial states of stress has been performed [1]. These tests were designed for the investigation of stress states with their principal directions being oblique to the principal material directions *L* (longitudinal) and *R* (radial to the stem). However, there is still a lack of experimental information with respect to the tangential direction (*T*) and knots. This is the motivation for planning additional test series in 2003.

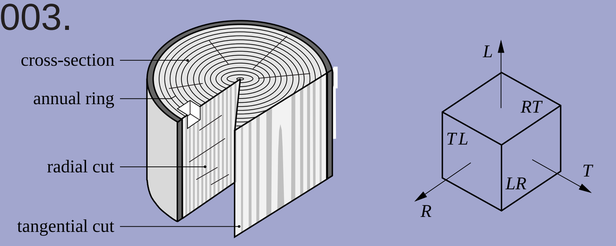

The influence of knots on the strength properties as well as the mechanical behaviour of the *T*-direction is necessary for realistic finite element ultimate load analyses of multiaxially loaded structural details as well as of shell structures made of wood. Results of these tests and attemptions for a elastic-plastic material model [2] shall be presented and discussed in this poster.

Literature: [1] Eberhardsteiner, J.: Mechanisches Verhalten von Fichtenholz - Experimentelle Bestimmung der biaxialen Festigkeitseigenschaften, Springer-Verlag, 2002.
[2] Mackenzie-Helnwein, P.; Eberhardsteiner, J. and Mang, H.A.: A Multi-Surface Plasticity Model for Clear Wood and its Application tothe Finite Element Analysis of Structural Details, Computational Mechanics, 31, 1-2, 204-218, 2003.

Experimental Setup

The test equipment consists of a biaxial servohydraulic testing apparatus for anisotropic materials and of a three-dimensional electronic Speckle Pattern Interferometer (ESPI) for the spatial deformation analysis of the measuring area of the plane specimen. Before testing, the specimens were stored at 20 °C and 65 % relative humidity until an equilibrium moisture content of *u* =12 % was reached.

a) Clear Spruce Wood

specimens for *LR*-plane and *LT*-plane

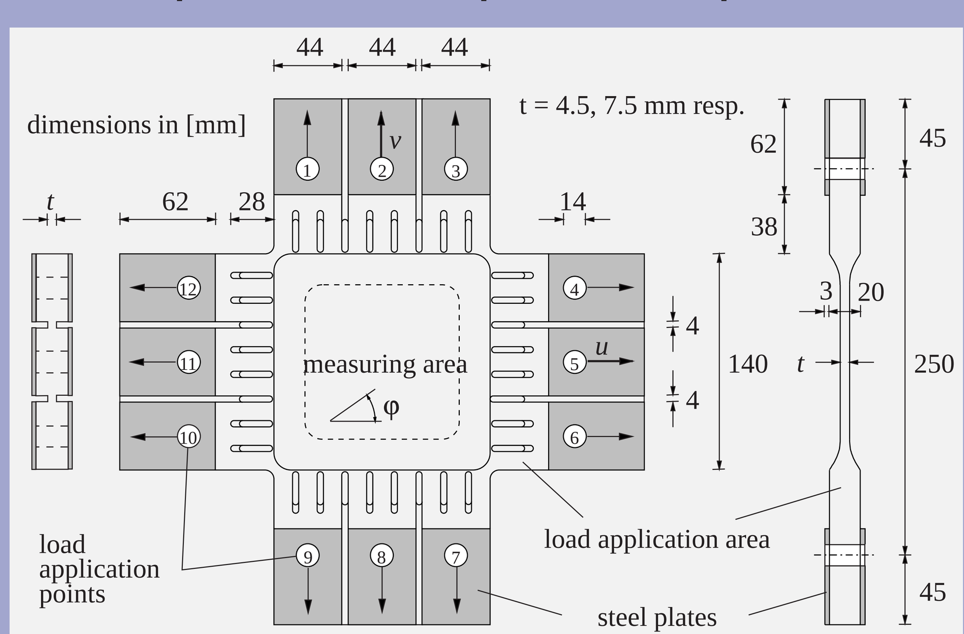

All experiments were performed under displacement control with different prescribed displacement rules depending on grain angle φ (measured to the horizontal axis) and biaxial load ratios κ = *u* : *v*.

b) Experiments with Knots

specimens for $L\overline{RT}$-plane for tension loading

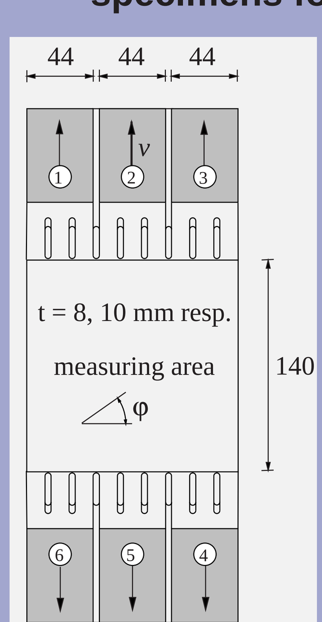

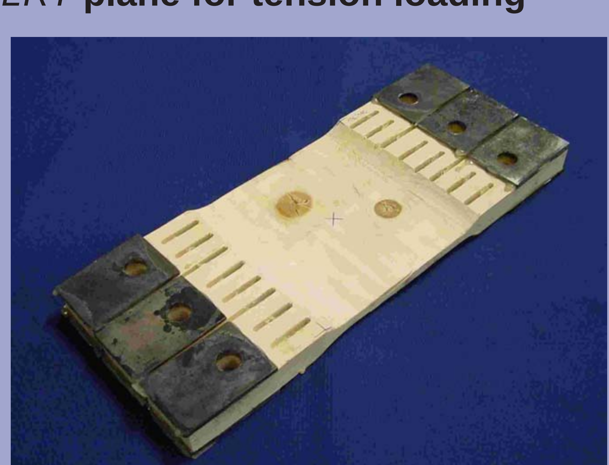

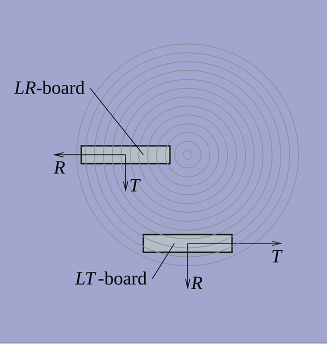

Knots are the commanding criterion of wood. This fact is inseparably combined with the deviation of the fibre direction around the knots. These influences on the failure strength (for tension loading) and on the yield stress (for compression loading), resp., will be investigated within a separate uniaxial test series.

Evaluation and Constitutive Modelling

Development of a Single-Surface Orthotropic Plasticity Material Model Including Hardening and Softening Behaviour for the $L\overline{RT}$-Plane

(Herbert MÜLLNER, Peter MACKENZIE-HELNWEIN)

Step 1 Clear Spruce Wood: *LR*-System

$$f = a_{LL}\sigma_L + a_{RR}\sigma_R + b_{LLLL}\sigma_L^2 + b_{RRRR}\sigma_R^2 + 2b_{LLRR}\sigma_L\sigma_R + 4b_{LRLR}\tau_{LR}^2 - 1 = 0$$

σ_L . . . stress in *L*-direction

σ_R . . . stress in *R*-direction

τ_{LR} . . . shear stress in the *LR*-plane

$a_{LL}, a_{RR}, b_{LLLL}, b_{RRRR}, b_{LLRR}, b_{LRLR}$ . . Tsai-Wu material parameters

Tsai-Wu yield surface and evolution laws

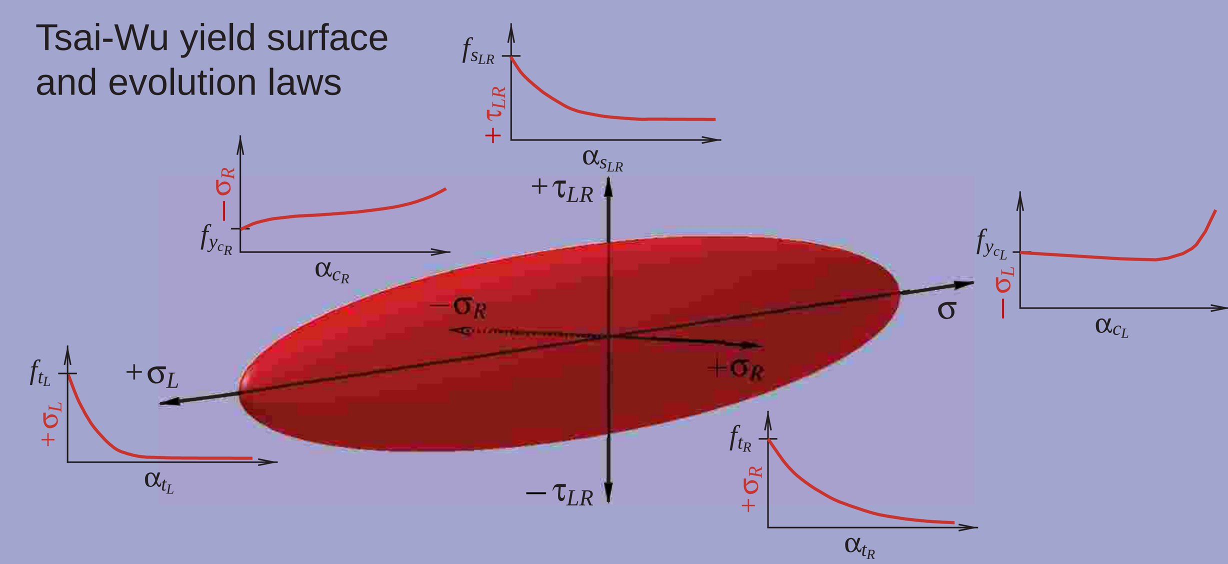

Step 2 Clear Spruce Wood: $L\overline{RT}$-System

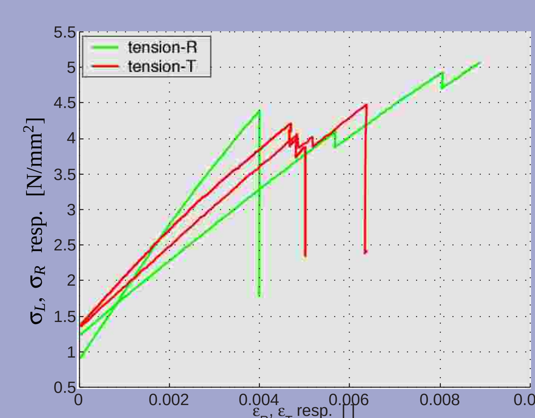

σε-diagr. for tension loading

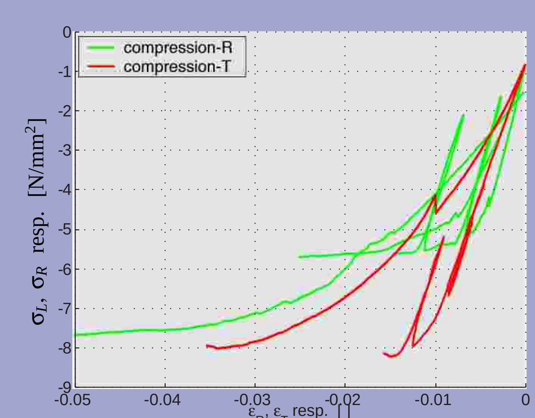

σε-diagr. for compression loading

cross section for gluelam lamellas

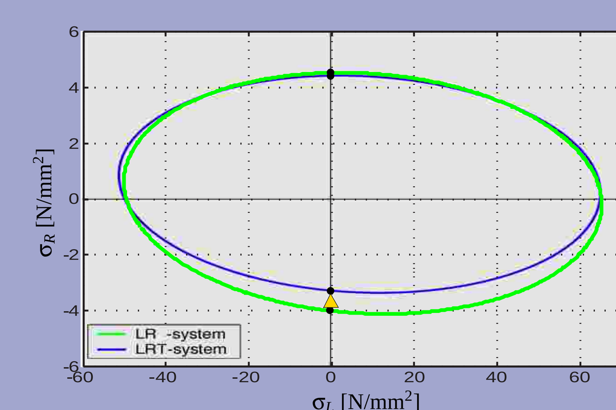

Tsai-Wu yield surface (*LR*-, $L\overline{RT}$-plane, resp.)

The cross sections of boards and scantlings, which are widely used in timber engineering, is characterised by fibre orientations in *R*- as well as in *T*-direction. Compared to the *L*-direction, the material behaviour in *R*- and *T*-direction is similar. Therefore, it is possible to reduce the mechanical behaviour in *R*- and *T*-direction to a $\overline{RT}$-equivalent.

$L = L$

$R \triangleright \overline{RT}$

Step 3 Include Knot Effects: Exemplary for Tension Loading in *L*-Direction

cross section of a board

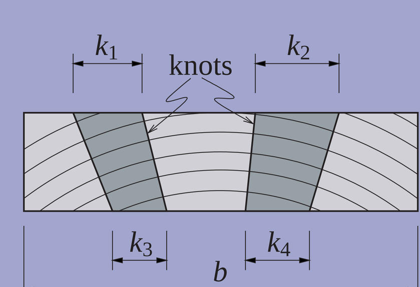

knot factor: $ksa = \frac{\sum_{i=1}^{n} k_i}{2b}$

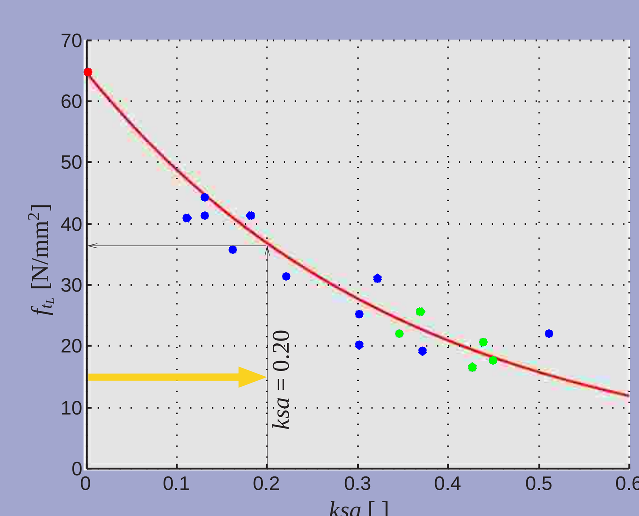

$f_{t_L}(ksa) = f_{t_{L,clear}} \cdot e^{rc \cdot ksa}$

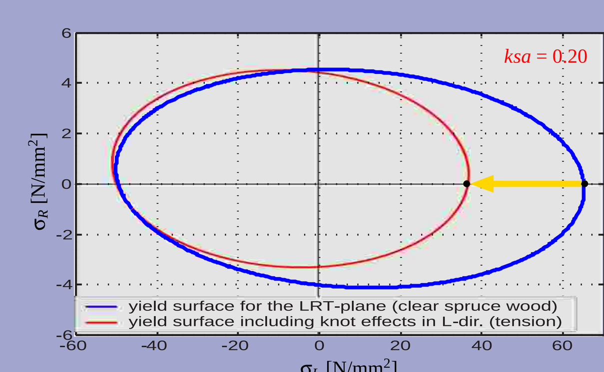

$f_{t_L}(ksa)$ . . . strength in *L*-dir. including knots

$f_{t_{L,clear}} = 65$ N/mm² . . . strength in *L*-dir. of clear wood

$rc = -2.82$ . . . regression coefficient

Example: Comparison Experiment - FEM (*LR*-Plane)

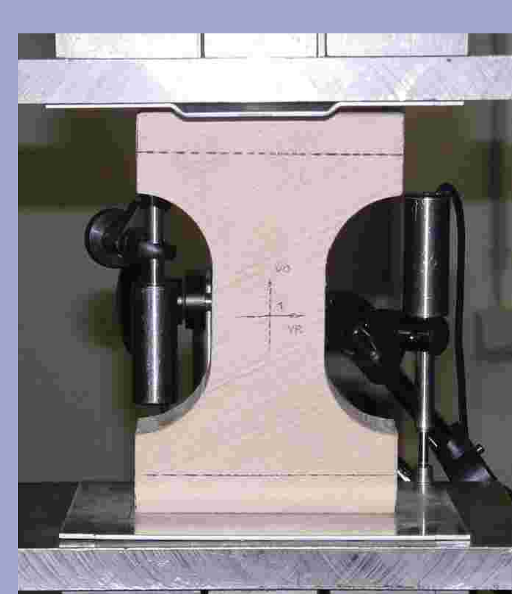

reference configuration

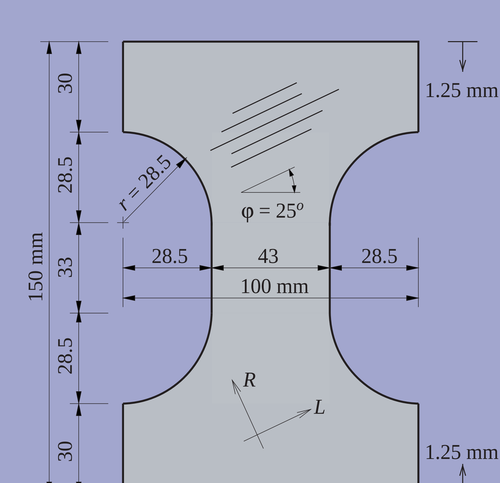

dimensions of the specimen

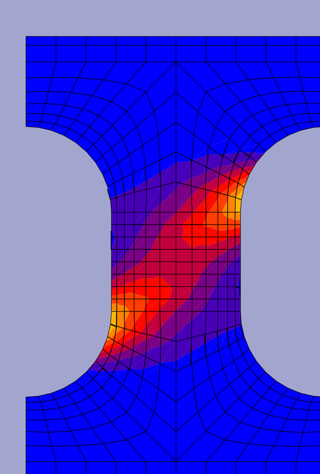

zones of plastic deformations

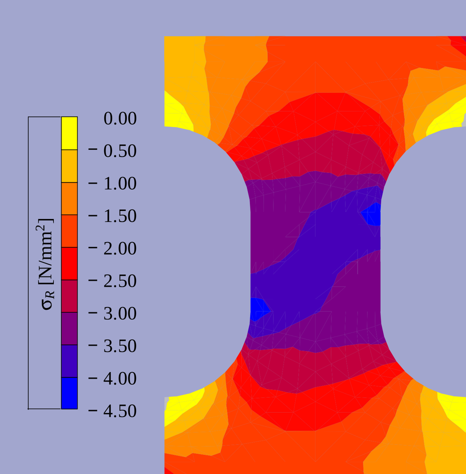

stresses in *R*-direction (test end, v = 2.5 mm)

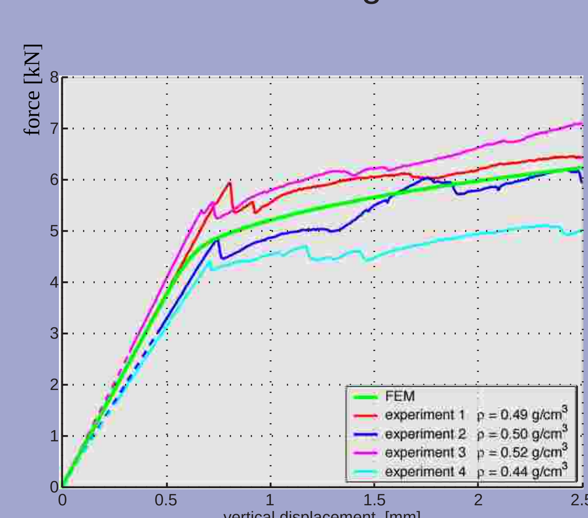

load-displacement diagram

used material parameter set:

$E_L = 9000$ N/mm²

$E_R = 500$ N/mm²

$\nu_{LR} = 0.50$

$G_{LR} = 450$ N/mm²

$f_{t_L} = 49$ N/mm²

$f_{yc_L} = -37$ N/mm²

$f_{t_R} = 3.4$ N/mm²

$f_{yc_R} = -3.0$ N/mm²

$\tau_{LR}^0 = 6.5$ N/mm²

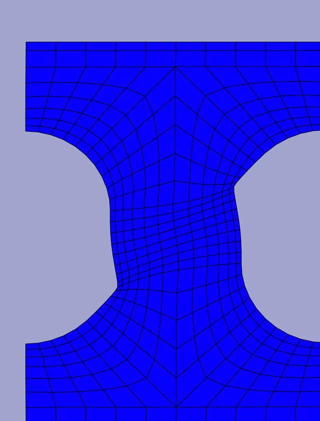

deformed configuration (scaling factor = 8)

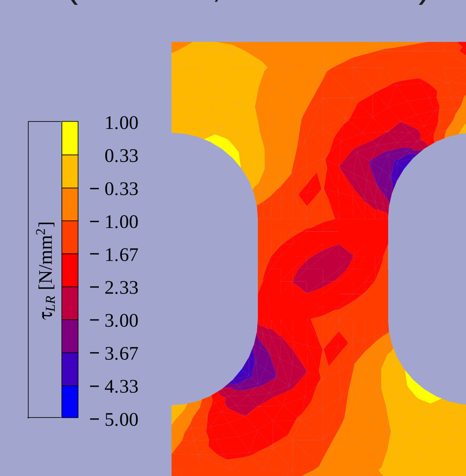

shear-stresses in the *LR*-plane (test end, v = 2.5 mm)